ELSEVIER

Materials Chemistry and Physics 72 (2001) 245–250

MATERIALS CHEMISTRY AND PHYSICS

www.elsevier.com/locate/matchemphys

Growth competition between crystalline silicon carbon nitrides and silicon nitrides deposited on Si wafer by MPCVD

Jin-Yu Wu, Cheng-Tzu Kuo*, Po-Ju Yang

Department of Materials Science and Engineering, National Chiao Tung University, 1001 Ta-Hsueh Road, Hsinchu 30050, Taiwan

Abstract

The Si–C–N films were synthesized on Si wafer by microwave plasma chemical vapor deposition with CH_4, N_2, 0.0–8.3 vol.% H_2 and the additional Si chips, as the sources. The growth competition on Si wafer between crystalline ternary Si–C–N and binary silicon nitrides was examined. Based merely on the results of ESCA, XRD and SEM analyses on the film surface, it might often give false impression of forming ternary silicon carbon nitride crystalline films, as reported in the literature, though their volume fractions of H_2 were from 35 to 77%. One of the possible reasons for a false impression is due to the fact that carbon often settles on the deposited films during cooling period. The further examinations on the cross-section of the films by TEM + EDS + ED, and on the film surface by FTIR and Raman spectroscopy clarify that the films essentially consist of ~2 μm binary silicon nitride crystals on top of ~100 nm ternary Si–C–N crystallites. This is in agreement with the ESCA depth profile examinations and the substrate scratching experiment by Si_3N_4 powders, which greatly enhance nucleation rate of binary silicon nitride crystals. Under a higher temperature and a longer deposition time, growth competition between crystalline Si–C–N and silicon nitrides will generally result in forming a film covered with silicon nitrides. The crystal structure of the silicon nitrides on the films is much close to α-Si_3N_4 than β-Si_3N_4 and tetragonal Si_3N_4 type structures, but silicon content is higher.

Keywords: Nitrides; Thin films; Plasma-assisted CVD; Electron microscopy; ESCA

1. Introduction

The carbon nitrides and silicon carbon nitrides were predicted to possess many useful properties, e.g. the highest hardness, semiconductor property and high efficient field emission, etc. [1–4]. Therefore, the synthesizing processes have attracted much attention, especially to deposit on Si wafer in order to link the Si technology for microelectronic applications. There were many methods to be claimed to deposit amorphous Si–C–N or crystalline silicon carbon nitride films, i.e., microwave plasma chemical vapor deposition (MPCVD) [5–9], magnetron sputtering [10], dual ion gun [11], pulse laser deposition (PLD) [12–14] and hot filament chemical vapor deposition (HFCVD) [14,15]. Among these proposed methods claiming to deposit the crystalline silicon carbon nitrides, the MPCVD have demonstrated the highest growth rate around 1 $\mu m\,h^{-1}$. They used the ESCA or AES results to claim the existence of ternary Si–C–N films, and the results of XRD or electron diffraction (ED) as the evidence of crystalline films. We also conducted the same analyses and MPCVD experiments, as proposed in the literature, except lower H_2 contents in the source gases. In addition, we use other analysis techniques to further characterize the film qualities, including TEM + EDS + ED, FTIR, Raman and ESCA depth profile. The motivation of this paper was to clarify the growth competition between crystalline ternary Si–C–N and binary silicon nitrides, and to examine the effect of deposition parameters, such as using additional Si sources and substrate scratching, on film nucleation and growth.

2. Experimental

The Si–C–N films were deposited on Si wafer by an MPCVD system with CH_4, N_2, 0.0–8.3 vol.% H_2 and Si chips as raw sources. Some of the substrates were subjected to Si_3N_4 powder scratching. The deposition conditions were as follows: CH_4/N_2 flow ratio 10/100 sccm/sccm; H_2/N_2 flow ratio either 0/100 or 10/100 sccm/sccm; microwave power 950 W; total pressure 15 Torr; substrate temperature 1100–1200 °C and deposition time 0.3–6 h. The deposited films were characterized by ESCA, ESCA depth profile, XRD, SEM, TEM + EDS + ED, FTIR and Raman spectroscopy.

* Corresponding author. Tel.: +886-3-5731949; fax: +886-3-5724727.
E-mail address: ctkuo@cc.nctu.edu.tw (C.-T. Kuo).

0254-0584/01/$ – see front matter
PII: S0254-0584(01)00446-1

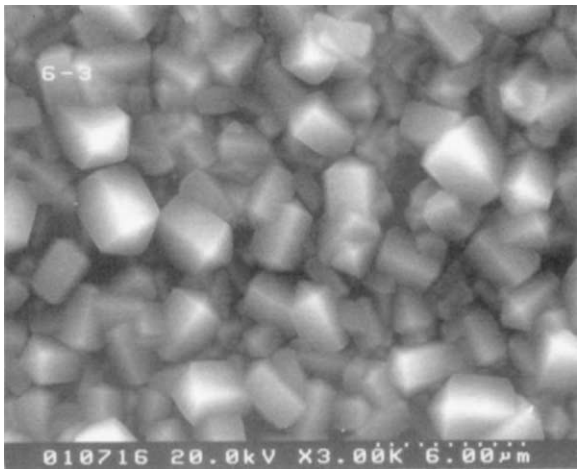

Fig. 1. Typical SEM micrograph of the film surfaces.

3. Results and discussion

3.1. Surface morphology, compositions and crystal structures of the films

The typical film morphology of the films is shown in Fig. 1, indicating crystalline facets of various grain sizes similar to the reported film morphologies in the literature. The surface compositions of the films as analyzed by ESCA indicate great fluctuation in values as follows: 16.1–40.2 at.% Si; 12.3–66.9 at.% C; 15.0–36.5 at.% N; 3.0–25.0 at.% O. As indicated later, formation of a thin layer of Si–C–N–O films can generally be found on the surface of the crystalline grains during the cooling stage after deposition. Compositions analyzed by ESCA are essentially the contents of the most top layer of the films, which may vary greatly depending on position, cooling condition and sputtering time before measurement.

The typical crystal structures as determined by XRD analyses are depicted in Fig. 2. It essentially shows the crystal structure of the top binary Si–N layer, because the Si–C–N layer is too thin in thickness and too small in grains to contribute to the diffraction peak intensity, as shown in next section. Fig. 2 indicates that the crystal structures match well with α-Si_3N_4 structure, and partially match with the β-Si_3N_4, and tetragonal Si_3N_4 type structures. As discussed later, based on the results of ESCA on compositions and XRD on crystal structure, we may give a false conclusion that the films consist mainly of new ternary crystals of Si–C–N. This may be the reasons why the same conclusion was made in the literature, though H_2 contents in the present conditions (either 0.0 or 8.3 vol.%) are lower than that in the literature (35–77 vol.%).

3.2. Film cross-section analyses

The typical TEM micrographs on the cross-section of the films are shown in Fig. 3(a) and (b). The micrographs can be roughly divided into three layers, i.e., Si–O, Si–C–N and Si–N layers, as indicated by the selected area EDS analyses. In Fig. 3, the most top Si–C–N–O thin layer of the films is not found. This is due to the fact that it is difficult to be differentiated with bonding materials for TEM specimen preparation, though the compositions can be detected by ESCA

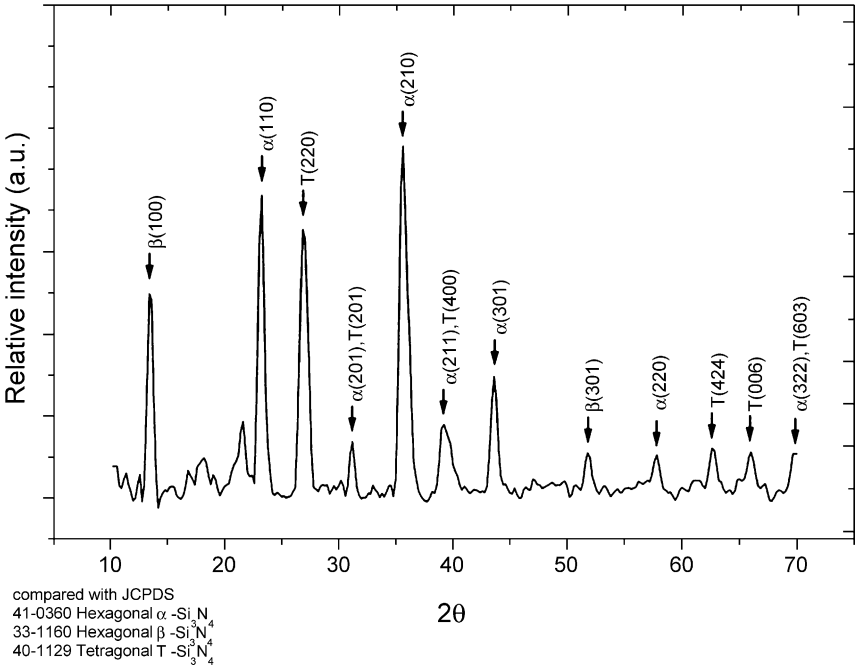

Fig. 2. Typical XRD pattern of the film surfaces.

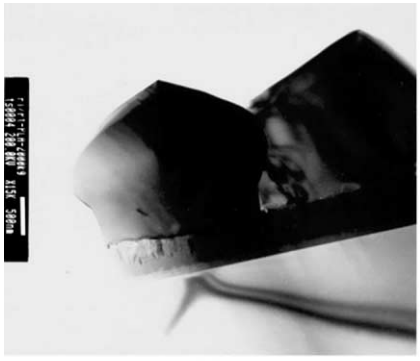

(a)

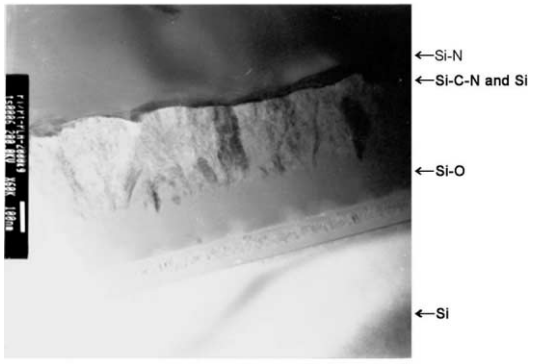

(b)

Fig. 3. Typical TEM micrographs of the cross-sections of the films: (a) 15k; (b) 60k magnifications.

on film surface, as indicated in the previous section. The oxygen content of the bottom Si–O layer at the substrate interface is roughly 28 at.%, which is the oxide layer of the Si wafer. The next Si–C–N layer is ∼100 nm in thickness and consists of mixtures of nano-crystalline grains of various compositions. It consists of pure Si grains and grains of various compositions (64.0–68.3 at.% Si + 9.0–16.3 at.% N + 9.7–22.8 at.% C). For a 6 h deposition time, the top Si–N layer consists of large crystals of ∼2 μm in size and with well-developed crystallographic facets. Their Si/N atomic ratios are ranging from 1.9 to 3.9, which are different from 0.75 for Si_3N_4 crystals. Under the present deposition conditions, the average growth rate ratio between Si–N and Si–C–N layers is ∼21/1.

The selected area ED analyses were also conducted for the Si–N and Si–C–N layers of the films, as presented in Figs. 4 and 5, respectively. Fig. 4(a) and (b) suggests that Si–N grains are single crystals with HCP crystal structure similar to various types of Si_3N_4 crystals. Fig. 5 indicates that the Si–C–N layer of the films is a polycrystalline material. Table 1 compares the $d_{(h\,k\,l)}$ spacing of various Si_3N_4 and SiC crystals from the literature with the calculated values for Si–C–N layer from ED patterns. It indicates that the crystal structure matches well with SiC crystal structure instead of Si_3N_4.

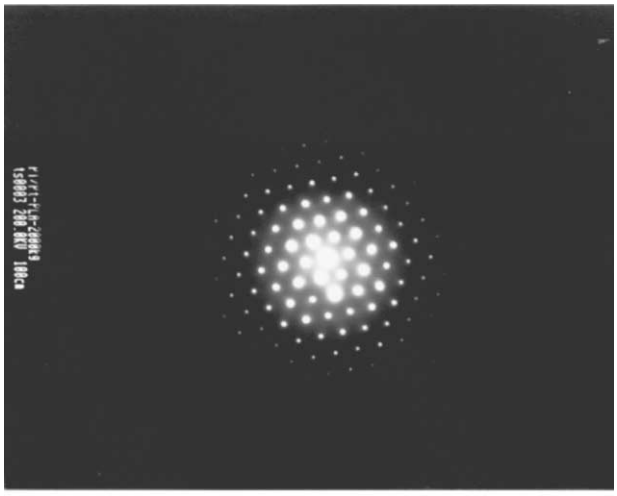

(a)

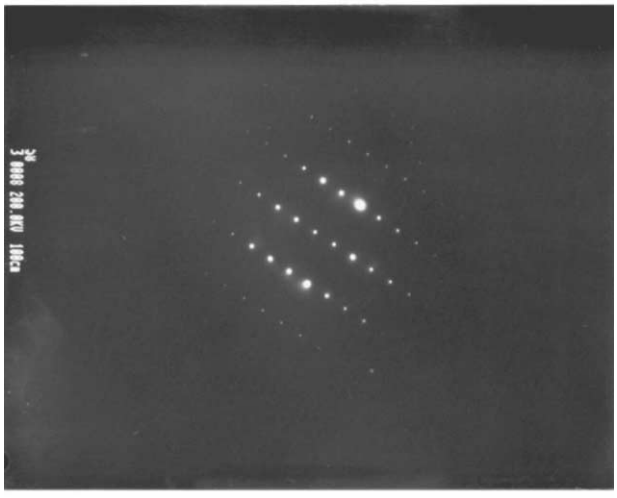

(b)

Fig. 4. The selected area ED patterns of one crystal in the Si–N crystal layer of the films with electron beam in: (a) ⟨0 0 1⟩; (b) ⟨2 2 3⟩ zone axis.

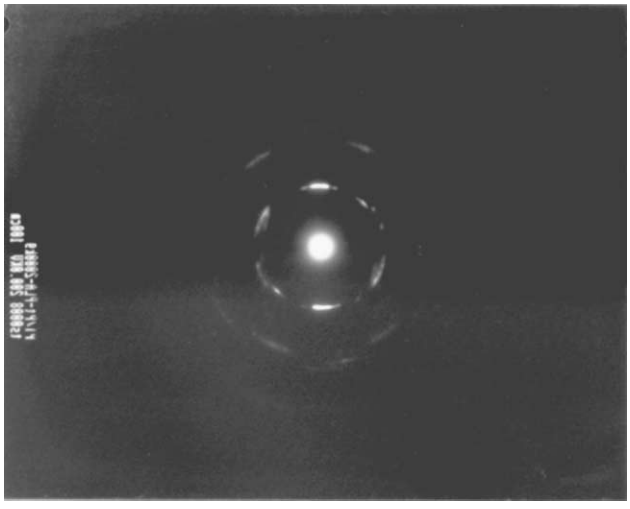

Fig. 5. The selected area ED pattern of the Si–C–N polycrystalline layer of the films.

Table 1
Comparison of the calculated $d_{(hkl)}$ spacings from ED analyses for Si–C–N layer with the values from the literature for various Si_3N_4 and SiC crystals

(hkl) plane	$d_{(hkl)}$ (Å)						
	Calculated	α-Si_3N_4[a]	β-Si_3N_4[a]	T-Si_3N_4[a]	α-SiC[b]	SiC[c]	SiC[d]
1 0 0	2.72573	6.71	6.583		2.67	2.669	2.669
0 0 2	2.57275	2.811	1.4534	4.2835			2.515
1 0 1	2.40123	4.3098	2.660		2.59	2.579	2.357
1 0 2	1.88861	2.593	1.4197	3.8292	2.36	2.357	1.8304
1 1 0	1.60082	3.877	3.8	6.5795	1.54	1.5407	1.5407
1 0 3	1.45739	1.8046	0.9589		2.08	2.088	1.4198
2 0 0	1.35190	3.359	3.293	4.6829		1.3343	1.3343
2 0 1	1.30299	2.883	2.1797			1.3227	1.2897
2 0 2	1.22096	2.155	1.3299		1.29	1.2897	1.1787
2 0 3	1.06160		0.9298		1.24	1.2398	1.0441
2 1 0	1.02910	2.538	2.489				1.0087
2 1 2	0.96973	1.8837	1.2554		0.98	0.98	0.9362
2 1 3	0.87545	1.5068			0.96		0.8643
3 1 0	0.75942	1.8627	1.8275				
3 1 2	0.72037	1.5521	1.1377				

[a] From JCPDS cards — 41-0360: hexagonal α-Si_3N_4; 33-1160: hexagonal β-Si_3N_4; 40-1129: tetragonal T-Si_3N_4.
[b] From JCPDS cards — 02-1462: hexagonal α-SiC.
[c] From JCPDS cards — 29-1127: hexagonal SiC.
[d] From JCPDS cards — 29-1126: hexagonal SiC.

The depth profile analysis of the films by analyzing the compositions as a function of the sputtering time is revealed in Fig. 6. It verifies that the most top layer consists of Si + C + N + O and the next top layer mainly Si–N (Si/N atomic ratio = 1.44, which is the same order in magnitude to EDS analyses) with traces O + C. This is in agreement with the previous TEM, EDS and ESCA analyses, though the quantitative values are not good enough.

The Raman spectroscopy reveals a broad peak between 1330 and 1580 cm^{-1}, indicating existence of C–C and C=C bonding structures near the surface. This is due to the fact that the Si–N bonding contributes no significant Raman scattering. The significant Raman signal is highly probable from the most top Si–C–N–O thin layer on the surface of Si–N crystals. In other words, the results from Raman spectroscopy are also in agreement with the TEM examinations.

3.3. Crystal bonding the films

The FTIR spectra of Si wafer and the films of 20 min and 6 h deposition times are shown in Fig. 7, which represent the initial and final growth stages of the films. There are Si–C, Si=C, Si=O bonds for films of 20 min deposition time, and mainly Si–N bond for films of 6 h deposition time. This is

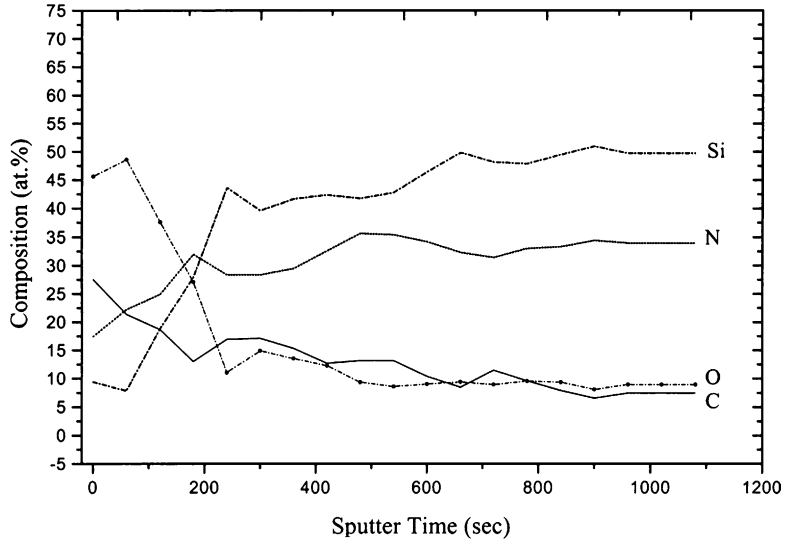

Fig. 6. Typical ESCA depth profile of the films.

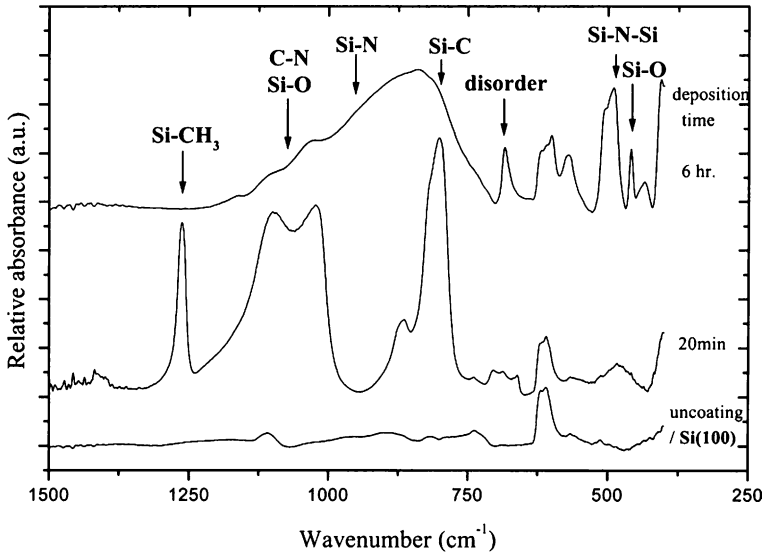

Fig. 7. FTIR spectra for Si wafer, films with 20 min and 6 h deposition times.

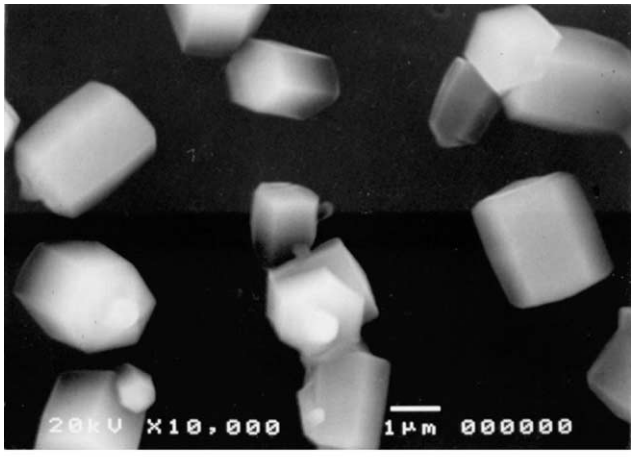

(a)

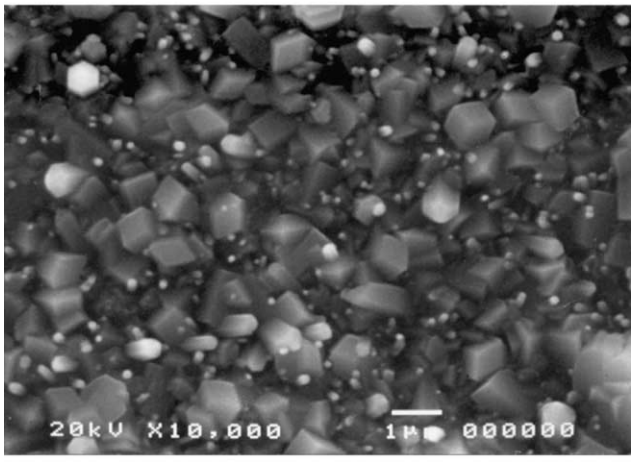

(b)

Fig. 8. SEM micrographs of the film surfaces: (a) substrate without scratching; (b) substrate scratching with Si_3N_4 powders before film deposition.

also in agreement with the previous results. The films of 20 min and 6 h deposition times corresponds to the Si–C–N and Si–N layers in Fig. 3, respectively. In other words, the Si–C–N layer can only be obtained in polycrystalline forms and during the initial stage of deposition. The larger crystals as reported in the literature or under our deposition conditions are mainly binary silicon nitrides instead of ternary silicon carbon nitrides.

3.4. Enhancement of film nucleation by Si_3N_4 powder scratching

To examine the effect of Si_3N_4 powder scratching on film deposition, nucleation densities of the films were compared with the films without substrate scratching. It results in a two-order of magnitude improvement in nucleation density, as shown in Fig. 8(a) and (b), respectively. The residues of Si_3N_4 powders appear to act as the effective seeds for nucleation of Si–N crystals. This signifies that the previous deposition conditions without substrate scratching are more favor conditions for the growth of binary silicon nitrides instead of ternary silicon carbon nitrides, as discussed in the previous sections.

4. Conclusions

The MPCVD method was intended to deposit the Si–C–N films on Si wafer with CH_4, N_2, H_2 and additional Si chips as the sources. The results show that the ternary Si–C–N films can only be formed at the initial stage of deposition. Under a higher temperature and a longer deposition time, growth competition between ternary Si–C–N crystals and binary silicon nitrides will generally result in forming a film

covered with silicon nitride crystals. The crystal structure of the silicon nitride layer is closer to α-Si_3N_4 than β-Si_3N_4 and tetragonal Si_3N_4 type structures, but silicon content is higher.

Acknowledgements

The Ministry of Education (contract No. 89-E-FA06-1-4) and the National Science Council of Taiwan (contact No. NSC89-2216-E009-020 and -019) supported this work.

References

[1] A.Y. Liu, M.L. Cohen, Science 245 (1989) 841.
[2] C.-Z. Wang, E.-G. Wang, Q. Dai, J. Appl. Phys. 83 (1997) 1975.
[3] L.C. Chen, C.K. Chen, S.L. Wei, et al., Appl. Phys. Lett. 72 (1998) 2463.
[4] A. Bendeddouche, R. Berjoan, E. Beche, R. Hillel, Surf. Coat. Technol. 111 (1999) 184.
[5] A. Badzian, T. Badzian, W.D. Drawl, R. Roy, Diam. Relat. Mater. 7 (1996) 1519.
[6] L.C. Chen, D.M. Bhusari, C.Y. Yang, et al., Thin Solid Films 303 (1997) 66.
[7] D.M. Bhusari, C.K. Chen, K.H. Chen, et al., J. Mater. Res. 12 (1997) 322.
[8] D.Y. Lin, C.F. Li, Y.S. Huang, et al., Phys. Rev. B 15 (1997) 6498.
[9] L.C. Chen, C.Y. Yang, D.M. Bhusari, et al., Diam. Relat. Mater. 5 (1996) 514.
[10] L.C. Chen, H.Y. Lin, C.S. Wong, et al., Diam. Relat. Mater. 8 (1999) 618.
[11] Z. He, G. Carter, J.S. Colligon, Thin Solid Films 283 (1996) 90.
[12] R. Machorro, E.C. Samano, G. Soto, L. Cota, Appl. Surf. Sci. 127–129 (1998) 564.
[13] W.F.A. Besling, A. Goossens, B. Meester, J. Schoonman, J. Appl. Phys. 83 (1998) 544.
[14] D.J. Jonson, Y. Chen, Y. He, R.H. Prince, Diam. Relat. Mater. 6 (1997) 1799.
[15] Z. Gong, E.-G. Wang, G.C. Xu, Y. Chen, Thin Solid Films 348 (1999) 114.